Uncovering the potentialities of protic ionic liquids based on alkanolammonium and carboxylate ions and their aqueous solutions as non-derivatizing solvents of Kraft lignin

Rafael M. Dias[a,b], André M. da Costa Lopes[b,*], Armando J.D. Silvestre[b], João A.P. Coutinho[b], Mariana C. da Costa[a]

[a] Department of Process and Product Design (DDPP) - School of Chemical Engineering (FEQ), University of Campinas (UNICAMP), Av. Albert Einstein, 500, Campinas, São Paulo, 13083-852, Brazil
[b] CICECO, Aveiro Institute of Materials, Department of Chemistry, University of Aveiro, 3810-193, Aveiro, Portugal

ARTICLE INFO

ABSTRACT

The present study scrutinized in depth the ability of alkanolammonium-based Protic Ionic Liquids (PILs) with carboxylate anions to dissolve Kraft lignin at 323.15 K. A focus was put on understanding the role of both PIL ions and water on the dissolution process. The results demonstrated that the anion plays a more important role in lignin dissolution than the cation. Furthermore, lignin dissolution was favored by increasing the alkyl chain of the carboxylate anion, while a smaller cation with lower number of hydroxyalkyl groups performed better. Among the studied solvents, the 2-hydroxyethylammonium hexanoate (HEAH) displayed the highest lignin solubility (37 wt%). In general, the addition of water had a negative influence on lignin solubility with the tested PILs. A sharp decrease in lignin solubility curves of 2-hydroxyethylammonium formate (HEAF) and acetate (HEAA) was observed, while a more softly effect was observed for 2-hydroxyethylammonium propionate (HEAP) and HEAH with the addition of water. However, a distinct behavior was observed for 2-hydroxyethylammonium octanoate (HEAO) that acted as hydrotrope enhancing lignin solubility in aqueous solutions to a maximum value at 40 wt% water content. Furthermore, by increasing the temperature, the lignin solubility was favored due to endothermic behavior of lignin dissolution process.

The dissolution of Kraft lignin was also performed at 393.15 K to unravel any lignin modification unleashed by PILs. GPC, FTIR-ATR and 2D NMR were employed for lignin characterization and the changes observed between native lignin and recovered lignin samples were negligible demonstrating the non-derivatizing character of the PILs. Moreover, the recycle of 2-hydroxyethylammonium propionate (HEAP) was successfully demonstrated for at least 3 cycles. In this way, PILs are herein revealed as promising solvents to apply in lignin valorization towards more efficient and eco-friendly processes.

1. Introduction

The current concerns about the environmental impact associated to fossil fuel consumption, the high energy demand and the growing need for commodities have been pushing the interest to use renewable resources, such as biomass, to provide biobased and sustainable products (Chang et al., 2017). In this context, the implementation of the biorefinery concept that relies on the use of biomass as feedstock to produce a wide range of biofuels, biobased chemicals and materials, has been attracting attention as a sustainable solution (Silveira et al., 2015).

Lignocellulosic biomass is a renewable and abundant resource comprising wood, agricultural and forestry residues, energy crops, cellulosic waste, among other streams. The worldwide production of these raw materials is estimated at 200 billion tons annually, making them suitable feedstocks for further processing and valorization (Dahmen et al., 2019). This type of biomass is composed of three major macromolecular components, namely cellulose (30–50 %) hemicelluloses (20–35 %) and lignin (15–30 %). The first two components make the polysaccharide fraction of biomass and assume a structural role in plant biomass, whereas lignin gives rigidity and protection against microbial attack. All these components are tightly bounded and organized in a rigid and complex structure hindering an efficient fractionation. Therefore, the chief challenge in biomass valorization lies on surpassing its recalcitrance and separating the macromolecular

---

* Corresponding author.
  E-mail address: andremcl@ua.pt (A.M. da Costa Lopes).

fractions for further conversion by efficient and sustainable methods (Da Costa Lopes and Bogel-Lukasik, 2015). In particular, the selective biomass delignification and lignin dissolution steps are key examples that must be improved towards an efficient lignin valorization. The aromatic nature of this macromolecule is of extreme importance for a forecasted replacement of aromatic chemicals and products coming from fossil-based resources (Hu et al., 2018).

Amongst biomass components, lignin is the less susceptible to chemical and biological treatments hindering its fractionation and conversion. Several technologies, including Kraft, soda, organosolv, microwave or ultrasound, have been applied in delignification and lignin dissolution processes. However, these technologies present low efficiency, high expenditures and some of them are not considered environmentally friendly, hampering their implementation to large-scale processes. The application of selective and benign solvents could be a more sustainable approach and ionic liquids (ILs) stand as promising green solvents for biomass delignification and lignin dissolution (Zhu et al., 2018).

ILs are organic salts with melting point below 373.15 K and are composed by cations and anions. They present remarkable features, such as non-flammability, negligible vapor pressure, high chemical and thermal stabilities, among others (Welton, 2018). Furthermore, physicochemical properties like density, viscosity and solvation power can be tailored by changing the anion or cation. For this reason, ILs are considered designer solvents to apply in a myriad of tasks (Welton, 2018). ILs can be roughly divided in aprotic ionic liquids (AILs) or protic ionic liquids (PILs) and can be distinguished by the permanency of the positive cation charge after synthesis. For AILs, the positive charge of the cation is kept, and it is not in equilibrium with the corresponding neutral species. The contrary is observed for PILs, in which charged and neutral species are present at equilibrium. PILs have the advantage of being easier to prepare, since a simple neutralization between a base and an organic acid is required.

The study of PILs as sustainable solvents for lignin dissolution and biomass delignification has been addressed by several authors. Merino et al. (2018) evaluated the ability of eighteen protic multiaromatic ILs for Kraft lignin dissolution. According to authors, 1,2,4,5-tetraphenyl-1H-imidazolium methanesulfonate ([TPIM][MeSO$_3$]) was able to dissolve 42 wt% lignin under microwave irradiation at 363.15 K (Merino et al., 2018). Rashid et al. (2016) examined the dissolution of Kraft lignin in three pyridinium PILs, namely pyridinium formate ([Py][For]), pyridinium acetate ([Py][Ac]) and pyridinium propionate ([Py][Pro]). The highest lignin solubility was obtained with [Py][For] at 348.15 K reaching a value of 70 wt% (Rashid et al., 2016). The good performance of this PIL was confirmed with the successful lignin extraction from palm oil plant biomass (Rashid et al., 2018). In another work, Achinivu et al. (2014) demonstrated the extraction of > 70 wt% of the initial lignin content from corn stover using pyrrolidinium acetate ([Pyrr][Ac]) without significant impact on cellulose fibers (Achinivu et al., 2014). More recently, Miranda et al. (2019) investigated 12 ammonium-based PILs to perform pineapple crown delignification. In particular, bis(2-hydroxyethyl)ammonium propionate [BHEAP] showed > 90 wt% lignin extraction, which clearly demonstrates the outstanding capacity of ammonium-based ILs for this purpose (Miranda et al., 2019).

The presence of water seems to have impact on delignification process using PILs. A high delignification yield (85 wt%) was achieved in the treatment of *Miscanthus giganteus* at 393.15 K with aqueous triethylammonium hydrogen sulphate ([TEA][HSO$_4$]) solution (20 wt% water content) (Brandt-Talbot et al., 2017). Similar results were achieved in sugarcane bagasse delignification using the same PIL aqueous solution (Chambon et al., 2018). Less effective delignification was attained with an aqueous solution of 1-butylimidazolium hydrogen sulphate [HBIM][HSO$_4$], which removed 35 wt% of the initial lignin content from cotton stalks (Semerci and Güler, 2018).

The state-of-the-art shows good results in the application of neat PILs or their aqueous solutions to dissolve lignin and to achieve efficient and sustainable biomass delignification. However, there is still lack of detailed knowledge regarding the mechanisms and interactions between lignin and PILs that take place during the dissolution process. The influence of both PIL cation and anion on lignin dissolution is a key factor that must be scrutinized as well as the impact of water on this process that is far from being understood. Furthermore, limited information regarding the structural modifications of the recovered lignin has been provided in literature. In this sense, the present work contributes to suppress all these gaps by giving a comprehensive understanding of the solubility of Kraft lignin (as a model macromolecule) in PILs aqueous solutions composed of alkanolammonium cations and carboxylate anions with different aliphatic chain lengths. Moreover, lignin was dissolved in PILs at high temperature to simulate conditions often applied in biomass delignification and recovered lignin was characterized in detail to unveil structural modifications triggered by those solvents. The recovery and reuse of PIL was also addressed in this work.

2. Experimental

2.1. Chemicals

All acid and base precursors employed for the synthesis of PILs examined in this work are represented in Fig. 1. The compounds 2-hydroxyethylamine (≥ 98 %), bis(2-hydroxyethyl)amine (≥ 98 %) and tris(2-hydroxyethyl)amine (≥ 98 %) were purchased from Sigma-Aldrich. Formic (≥ 98 %) and acetic acids (> 99 %) were purchased from Merck. Propionic acid (≥ 99 %) was purchased from Acros Organics, while hexanoic (≥ 98 %) and octanoic acid (≥ 98 %) were supplied by Sigma Aldrich. All reagents were used as purchased.

Kraft lignin from *E. globulus* was directly supplied by Suzano Papel & Celulose (Brazil) after employing carbon dioxide (CO$_2$) to the industrial black liquor.

2.2. PILs synthesis and characterization

The following PILs were synthesized: 2-hydroxyethylammonium formate (HEAF), 2-hydroxyethylammonium acetate (HEAA), 2-hydroxyethylammonium propionate (HEAP), 2-hydroxyethylammonium hexanoate (HEAH), 2-hydroxyethylammonium octanoate (HEAO), bis(2-hydroxyethyl)ammonium propionate (BHEAP) and tris(2-hydroxyethyl)ammonium propionate (THEAP).

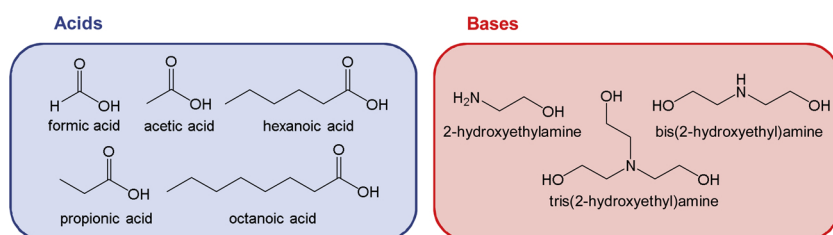PILs were prepared according to the methodology described by

Fig. 1. Acid and base precursors used in this work to perform PILs synthesis.

Álvarez et al. (2010) and Iglesias et al. (2010). The amine was placed inside a three-necked flask equipped with a reflux condenser, a PT-100 temperature sensor for monitoring the temperature and a dropping funnel. Since the reaction is exothermic, a thermostatic bath (283.15 K) covering the three-necked flask was needed to avoid temperature increase during the reaction. The organic acid (formic, acetic, propionic, hexanoic or octanoic) was added dropwise to the flask and the solution was continuously stirred with a magnetic bar up to 24 h at room temperature. No solid precipitate or crystals in the mixture were observed during PILs' synthesis. PILs were then submitted to vacuum (70.0 Pa absolute pressure) with slight heating (333.15 K) and agitation to remove water and excess of reagents. The water content was measured after this step using a Metrohm 831 Karl Fischer coulometer and determined values were considered in the preparation of PILs aqueous solutions.

The success of PILs synthesis was confirmed by FTIR-ATR analysis and by both ^{1}H NMR and ^{13}C NMR techniques (Figs S1–S21 in electronic supporting information - ESI).

2.3. Lignin solubility assays

Kraft lignin in excess amount was added to 1.0 $\pm$ 0.05 g of each PIL aqueous solution (10, 25, 40, 50, 60, 75, 80, 85 and 97 wt%) or pure water in glass vials. The vials were sealed and placed on a specific aluminum disk support, which was transferred to a stirring plate with heat control Pt1000 (H03D Series from LBX Instruments). The solubility assays were performed at 323.15 K under constant agitation of 200 rpm. After saturation was reached, the samples were filtered using PTFE filters (0.45 μm pore size) allowing separation of the undissolved lignin from the liquid phase. Afterwards, the liquid phase was diluted with dimethylsulfoxide (DMSO) and the amount of dissolved lignin was quantified by UV-spectroscopy (SHIMADZU UV-1700, Pharma-Spec spectrometer) at a wavelength of 280 nm. Quantitative determination was assisted by appropriate calibration curves (Table S1 in ESI). All experiments were performed at least in duplicate and results were expressed as means (less than 5% variation).

2.4. Lignin recovery and PIL recycling

Deionized water was added to lignin/PIL solution and stirred for lignin precipitation. The solution was then introduced in an ice bath (278.15 K) to increase the efficiency of precipitation. The recovered lignin was separated by vacuum filtration and washed with deionized water to ensure that all PIL has been washed out. Precipitated lignin was dried under vacuum at 303.15 K for 24 h and the amount of lignin was determined gravimetrically. The resulting PIL aqueous solution from washing step was collected for recycle/reuse purposes. The solution was submitted to a simple distillation process at ambient pressure to remove major water fraction. Afterwards, the resulting solution was submitted to a vacuum evaporation process (333.15 K and 10 kPa) until approximately 15 wt% water content was achieved. The remaining PIL aqueous solution was reused in lignin solubility assays as described in Section 2.3.

2.5. Gel permeation chromatography (GPC)

Gel Permeation Chromatography was carried out with a PL-GPC 110 chromatograph (Polymer Laboratories, UK) equipped with two columns PL gel MIXED-D 5 μm (300 x 7.5 mm) protected by a PL aqua gel-OH Guard 5 μm pre-column. The columns, injector system and the detector (RI) were maintained at 343.15 K during the analysis. A solution of LiCl in dimethylformamide (0.1 mol L^{-1}) was prepared and used as eluent. Lignin samples were dissolved in the eluent solution to a concentration of about 1 wt% (10 mg mL^{-1}). The injection volume of samples was 100 μL and the eluent was pumped at a flow rate of 0.9 mL min^{-1}. The analytical columns were calibrated with lignin model compounds

(monomer, dimmer and tetramer) with known molecular weight in the range of 1–4 kDa. The following equation was determined as the calibration curve: LogM = 6.283 − 0.2149 * T.

2.6. Fourier transform infrared analysis (FTIR-ATR)

FTIR spectra of PILs and lignin samples were acquired by a Perkin Elmer spectrometer (Spectrum BX) equipped with a single horizontal Golden Gate ATR cell (attenuated total reflectance) and a diamond crystal. The data was recorded with 32 scans at a resolution of 4 cm^{-1} and a wavenumber range between 4000 cm^{-1} and 600 cm^{-1}.

2.7. Nuclear magnetic resonance (NMR) spectroscopy

2.7.1. ^{1}H and ^{13}C NMR

The ^{1}H and ^{13}C NMR spectra of ILs were recorded by a Bruker AVANCE 300 MHz NMR at 300.13 MHz and 75.47 MHz, respectively, using deuterated dimethylsulfoxide (DMSO-d6) as solvent and tetramethylsilane (TMS) as the internal reference.

2.7.2. 2D HSQC NMR

In sample preparation, 50 mg of lignin was dissolved in 500 μL of DMSO-d6 with TMS as the internal reference and transferred to NMR tubes. 2D HSQC NMR spectra were acquired by a Bruker AVANCE 500 MHz NMR spectrometer equipped with an inverse gradient 5 mm TXI ^{1}H/^{13}C/^{15}N cryoprobe. ^{1}H–^{13}C correlation spectra were measured with the following Bruker standard pulse program: "hsqcetgpsi" sequence with 2D H-1/X correlation via double inept transfer (trim pulses), Echo/Antiecho-TPPI gradient selection for phase sensitivity improvement, and decoupling during acquisition. The chemical shifts were referenced to the central DMSO solvent peak (δC 39.5 ppm, δH 2.49 ppm). All the experiments were carried out at 298.15 K with the following parameters: spectral width of 11 ppm in the F2 (^{1}H) dimension and 165 ppm in the F1 (^{13}C) with 1024 data points, 194 scans and recycle delay of 1.5 s.

For semi-quantitative analysis, phase and baseline correction were performed to all HSQC spectra. The relative abundance of main inter-unit linkages and lignin substructures was determined as the percentage of total side chains from integration of ^{13}C-^{1}H cross signals in the HSQC spectra.

3. Results and discussion

3.1. The influence of water and PIL cation on lignin solubility

The presence of water in IL decreases its viscosity, reduces the amount of IL required for a dissolution process and saves costs in IL production (and recycling), since an energy-intensive drying step would be avoided. Therefore, the influence of water on the ability of PILs to dissolve lignin should be comprehensively scrutinized.

The importance of water and PIL cation in the solubility of Kraft lignin was first evaluated. Neat and aqueous solutions of HEAP, BHEAP and THEAP that share propionate anion were examined for Kraft lignin dissolution. The solubility values as function of PIL water content at 323.15 K are presented in Fig. 2 and Table S2 (ESI).

At first glance, the results showed a negative impact of water on the performance of PILs to dissolve Kraft lignin, *i.e.*, the higher water content, the lower is the solubility of lignin in the solvent. Adding water to PILs between 15.0 wt% and 75.0 wt% sharply decreases lignin solubility in all cases and when water content becomes higher than 75.0 wt%, lignin solubility is < 2.0 wt%. This trend was also observed in the Kraft lignin solubility with pyridinium-based PILs reported by Rashid et al. (2016). It is an expected behavior since water is usually employed as lignin anti-solvent in biomass fractionation processes with ILs (Brandt et al., 2015; Prado et al., 2013).

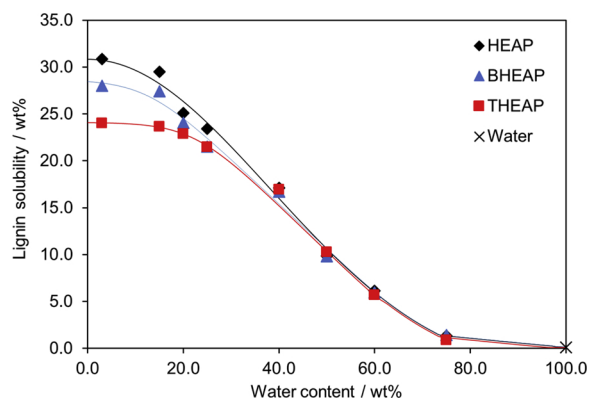Regarding the PILs performance, HEAP depicted higher ability to

Fig. 2. Kraft lignin solubility (wt%) in HEAP, BHEAP, THEAP and their aqueous solutions at 323.15 K. Lines are guide for the eye.

dissolve Kraft lignin than BHEAP and THEAP for water contents ≤ 25 wt%. This can be attributed to the number of hydroxyalkyl chains in cation structure and the cation size as well. These factors seem to influence the lignin solubility for neat PIL and PIL aqueous solutions at low water content, in which lignin solubility is favored by a smaller cation size and a lower number of hydroxyalkyl groups provided by HEAP. The steric hindrance provided by higher number of carbon chains and cation size might occur and the lignin-cation interaction could be reduced, which may explain the decrease in lignin solubility (Hart et al., 2015).

However, no relevant differences were observed between the PILs for water content higher than 40 wt%. This means that adding water to these PILs at a certain point masks the influence of IL cation mentioned above, and thus, it can be concluded that the PIL cation plays a minor role in lignin solubility. This is also corroborated by results of several previous works that showed a major influence of IL anionic part on lignin solubility (Achinivu, 2018; Ji et al., 2012; Merino et al., 2018; Pu et al., 2007; Zhang et al., 2017).

3.2. The influence of PIL anion on lignin solubility

The impact of PIL anion on lignin solubility was also studied and 2-hydroxyethylammonium cation was chosen as reference to the detriment of other cations that presented lower performance. The solubility of Kraft lignin was tested in five PILs (neat and aqueous solutions) composed of anions with different alkyl chain length, namely formate (HEAF), acetate (HEAA), propionate (HEAP), hexanoate (HEAH) and octanoate (HEAO) at 323.15 K. The solubility results are depicted in Fig. 3 and Table S3 (ESI).
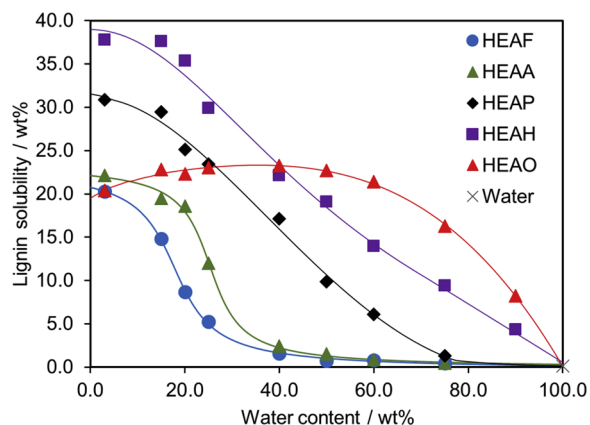

Fig. 3. Kraft lignin solubility (wt%) in HEAF, HEAA, HEAP, HEAH and HEAO their aqueous solutions at 323.15 K. Lines are guide for the eye.

The ability of neat PILs to dissolve lignin can be ordered as the following: HEAH > HEAP > HEAA > HEAF ≈ HEAO. Among examined PILs, HEAH stand as the best lignin solvent achieving a solubility value of 37.77 wt% at 323.15 K, which is similar to Kraft lignin solubility in other solvents at similar or even higher temperatures (Achinivu, 2018; Hart et al., 2015; Merino et al., 2018; Pu et al., 2007; Soares et al., 2019). Imidazolium-based ILs were tested by Pu et al. (2007) and Hart et al. (2015), and the best ILs were found to dissolve 344 g/L of Kraft lignin at 323.15 K, and 55 wt% of Kraft lignin at 298.15 K, respectively. Merino et al. (2018) evaluated several multi-aromatic PILs for kraft lignin dissolution task, achieving 42 wt% of solubility at 363.15 K, while Soares et al. (2019) demonstrated that aqueous solutions of DES formed by propionic acid:urea (2:1) reached more than 27 wt% of kraft lignin solubility at 353.15 K. The results obtained in this study evidence the strong capacity of these PILs to dissolve lignin at mild conditions (323.15 K), and are fairly comparable with AILs (Hart et al., 2015; Pu et al., 2007), other PILs (Achinivu, 2018; Merino et al., 2018), and also DES aqueous solutions (Soares et al., 2019).

When water is added to PILs different trends in lignin solubility were observed. For PILs with short alkyl chain anions (formate and acetate), the negative influence of water on lignin solubility is even higher than that observed for HEAP and HEAH. A sharp decrease of lignin solubility is achieved to water contents between 15.0 wt% and 40.0 wt% for HEAF and HEAA, while it softly decreases for both HEAP and HEAH at the same range of water content. Some authors have also reported the negative effect of water on lignin dissolution using ILs (Akiba et al., 2017; Rashid et al., 2016; Xu et al., 2017). According to Xu et al. (2017), the water crowd the hydrogen bond accepting sites of IL anions and impairs the interactions between lignin and ILs, resulting in the reduction of PILs dissolution ability (Xu et al., 2017). Theorical calculations were performed by Ji et al. (2012) to investigate the interactions between lignin-water-ILs. The authors have concluded that the active sites and the interaction energy of ILs-lignin are impaired by the presence of water making the bonds weaker or disrupted (Ji et al., 2012). However, there are some cases in which water does not significantly decrease the lignin solubility, as can be seen for HEAH, up to 15 wt% water content. This behavior was not observed for any other PIL studied. It is also surprising that 4.35 wt% lignin solubility was reached at highly diluted HEAH solutions (90 wt% water). Therefore, a higher alkyl chain length of the carboxylate anion allows a better affinity for lignin dissolution and the anti-solvent role of water is reduced, at least up to a six-carbon chain length. This is in agreement with lignin solubility results achieved with cholinium-based ILs containing different chain length alkanoate anions as reported by Hou et al. (2015). However, an opposite conclusion was disclosed by Rashid et al. (2016) when performing lignin solubility trials with pyridinium-based ILs. The researchers showed pyridinium formate as the best performing IL for lignin dissolution in comparison with the acetate and propionate counterparts (Rashid et al., 2016). Nevertheless, it is important to highlight that the same study also shows that molecular pyridine can reach a lignin solubility more than twice as that observed for formic acid (Rashid et al., 2016). Therefore, pyridinium cation may play a major role in lignin solubility in these type of ILs, which is explained by the π–π interactions established between IL cation and lignin aromatic rings. All these results lead us to conclude that the combination of IL cation and anion interferes with the individual role of each IL component in lignin dissolution.

On the other hand, a remarkably different behavior was observed for octanoate-based PIL (HEAO). As can be seen in Fig. 3, lignin solubility in neat HEAO is almost half of that observed for neat HEAH. In aqueous solutions, it can be noted that HEAO dissolves more lignin than other PILs for water contents > 40 wt%, reaching 23.27 wt% maximum lignin solubility. But suddenly, lignin solubility reduces in solutions containing higher water content. Indeed, the shape of the lignin solubility curve of HEAO is characterized by a maximum between pure

water and neat HEAO, suggesting that the solubility of lignin in this case is driven by a hydrotropic mechanism. Basically, the HEAO ions self-arrange in water and act as hydrotrope enhancing lignin solubility in aqueous solutions. This phenomenon was previously reported in the dissolution of phenolic compounds in IL aqueous solutions by Cláudio et al. (2015) and in the dissolution of lignin monomeric model compounds in deep eutectic solvent aqueous solutions by Soares et al. (2017).

Hence, it was demonstrated that increasing alkyl chain length of the anion in ethanolammonium-based ILs enhances lignin solubility, while water acts as lignin anti-solvent. This means that the hydrophobicity of the anion could play a positive role in lignin dissolution and, at certain point, the dissolution mechanism changes as consequence of the self-arrangement of amphiphilic IL anions (e.g. octanoate) around lignin macromolecules increasing its solubility in aqueous solutions.

Although water decreases lignin solubility, the use of PIL aqueous solutions at low water content (e.g. 15 wt%) may be beneficial for certain purposes, as for example, in biomass delignification processes. As shown elsewhere (Brandt-Talbot et al., 2017), 20 wt% water content improved the efficiency of [TEA][HSO$_4$] to extract lignin from *Miscanthus giganteus* reaching > 85 wt% delignification yield at 393.15 K. The low amount of water reduces the PIL viscosity, improving lignin extraction yields. Water is thus important to improve mass transfer during lignin extraction, but a low water content is desirable to not significantly affect lignin solubility.

3.3. The effect of temperature on lignin solubility

The HEAP was chosen, as proof of concept, to evaluate the influence of temperature in lignin solubility. The dissolution of lignin in HEAP aqueous solutions was evaluated at 313.15, 323.15, 333.15, and 353.15 K (Fig. 4 and Table S4).

In general, the same trend was observed to all solubility lignin curves: the lignin solubility softly decreases with the addition of water, as mentioned before. The increase of temperature favored the lignin dissolution as a result of the kinetic energy increase, allowing PIL molecules to break apart easily the lignin molecules enhancing the solubility. This behavior is in agreement with the general solubility rule (endothermic processes) (Fathi-Azarjbayjani et al., 2016; Kim et al., 2018; Long et al., 2017). A maximum lignin solubility of 38.15 wt% was observed in neat HEAP at 353.15 K.

Some authors have reported ILs ability to dissolve Kraft lignin at different temperatures. Glas et al. (2015) screened a series of ammonium-, phosphonium-, and pyrrolidinium-based ILs and achieved 460 g/L lignin solubility at 363.15 K using tributylmethylphosphonium methylsulfate ([P4441][MeSO$_4$]) as solvent medium. Mu et al. (2015) synthesized and tested several ILs formed by *N*-methyl-2-pyrrolidone

and carboxylic acids and reported that this kind of ILs can reach 35–60 wt% of lignin solubility at 363.15 K. Regarding the ability of PILs to dissolve Kraft lignin, Rashid et al. (2016) achieved more than 70 wt% of lignin solubility using pyridinium formate ([Py][For]) at 348.15 K. Therefore, HEAP presents good capacity to dissolve Kraft lignin when compared with literature data (Glas et al., 2015; Mu et al., 2015; Rashid et al., 2016; Soares et al., 2019).

3.4. Structural characterization of lignin submitted at high temperature in PILs

After careful evaluation of the potentialities of examined PILs to dissolve lignin at 323.15 K, a comprehensive lignin characterization was performed. At this stage, lignin was dissolved in neat PILs at 393.15 K for 6 h followed by its precipitation with water. These conditions were intended to simulate those usually applied in biomass delignification processes and to unveil any structural modification in lignin induced by PILs. A series of techniques, including GPC, FTIR-ATR and 2D-NMR were performed for the analysis of native Kraft lignin and recovered lignins. Given the limited technical resources and time consuming of analyses, recovered lignins from HEAF, HEAP and THEAP media were selected as representative samples to screen the influence of the PIL ions on lignin modification.

The impact of selected PILs on lignin molecular weight was first evaluated. The weight average molecular weight (Mw), the number average molecular weight (Mn) and the polydispersity index (PDI) of native Kraft lignin and recovered lignins from HEAF, HEAP and THEAP are presented in Table 1. The corresponding molecular weight distributions of all lignin samples are presented in Fig. S23 (in ESI).

The GPC data revealed a native Kraft lignin characterized by low molecular weight and narrow molecular weight distribution (low polydispersity). The process of Kraft pulping is in general a severe process, thus a drastic reduction of lignin molecular weight is expected (Hu et al., 2018). Contrasting to literature, the obtained values are consistent with those reported for *E. globulus* Kraft lignins (Tolbert et al., 2014). On the other hand, the thermal treatment of this lignin in PILs demonstrated a slight increase of Mw, Mn and PDI values in all cases. Hence, low chemical modification in lignin occurred or simply low molecular weight lignin fractions (oligomers) remained solvated after dissolution/precipitation steps. In order to better sort out these effects and to address any chemical modifications in recovered lignins, FTIR-ATR and 2D-NMR analyses were performed.

The acquired FTIR spectra of native Kraft lignin and recovered lignins after dissolution in HEAF, HEAP or HTEAP are presented in Fig. 5. The samples were analyzed according to lignin infrared characterization reported in literature (Cachet et al., 2014; Cademartori et al., 2013; García et al., 2012; Gordobil et al., 2015; Nevrez et al., 2011; Pandey and Pitman, 2003; Sun et al., 2012). Typical Kraft lignin absorption bands were observed in the region of 1800–750 cm^{-1} with remarkable high intensities at 838, 1109, 1212, 1327, 1456, 1514, 1600 and 2937 cm^{-1}. The characteristic lignin assignments are presented in detail in Table S5 (ESI).

The spectra of the native Kraft lignin and recovered lignins are comparable and only minor differences are noticeable. No extra vibrational bands were observed in spectra of HEAF and HEAP lignins,
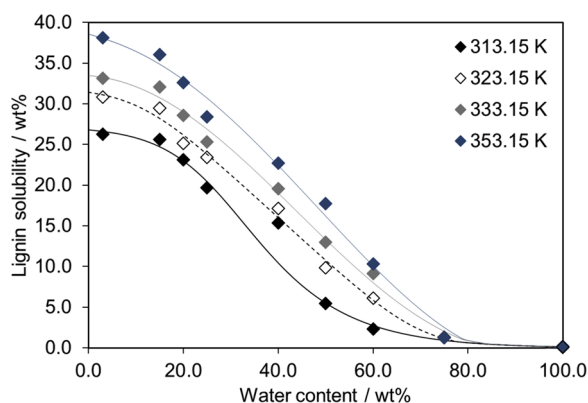

Fig. 4. Kraft lignin solubility (wt%) in HEAP aqueous solutions and in pure water at 313.15, 323.15, 333.15 and 353.15 K. Lines are guide for the eye.

Table 1
Calculated molecular weight numbers of native Kraft lignin and recovered lignin samples achieved by GPC analysis.

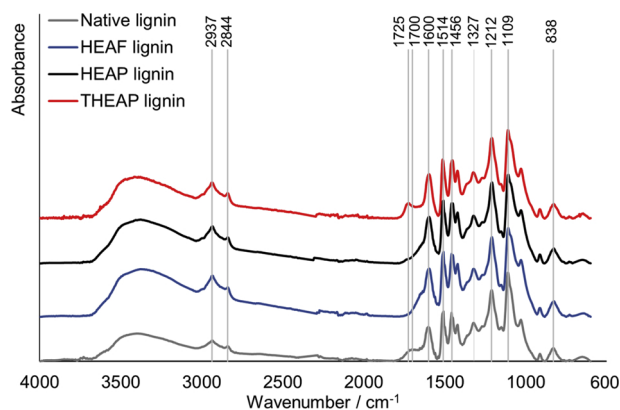| Lignin Sample	Mw (g mol^{-1})	Mn (g mol^{-1})	PDI
Native Kraft	1520	1345	1.13
HEAF	1725	1465	1.18
HEAP	1600	1395	1.15
THEAP	1650	1440	1.15

Fig. 5. FTIR-ATR spectra of native Kraft lignin and recovered lignins from HEAF, HEAP and THEAP. Recovered lignins were obtained after dissolution in PILs at 393.15 K and further precipitation with water.

but a band at 1700 cm^{-1} seems to disappear in these samples. This band can be attributed to C=O stretching in conjugated carbonyl groups present in lignin structure (Cachet et al., 2014), but also to moisture (water bending vibration) and protein impurities (Popescu et al., 2006) that could be removed after PIL treatment. On the other hand, the appearance of vibrational band at 1725 cm^{-1} is highlighted only in THEAP lignin spectrum that could be associated to C=O stretching in ester groups. Overall FTIR analysis showed small modifications in lignin chemical linkages and functional groups, but this technique alone gives limited and inconclusive information. Therefore, a more in-depth structural analysis was performed with 2D HQSC NMR technique.

Each lignin HSQC spectrum can be divided in three distinct regions, namely aliphatic side chain (δ_C/δ_H 5.0–35/0.5–2.5), oxygenated aliphatic side chain (δ_C/δ_H 50–95/2.5–5.0) and aromatic (δ_C/δ_H 100–135/6.0–8.5) regions (Fernández-Costas et al., 2014; Ralph and Landucci, 2010). The nonoxygenated aliphatic side chain region presents signals of lipids, degraded products of lignin and other organic contaminants that hinders a suitable analysis (Ibarra et al., 2007; Liitiä et al., 2003). Therefore, a higher focus was given to oxygenated aliphatic and aromatic regions. For example, these spectra regions of native Kraft lignin and HEAP lignin are depicted in Fig. 6.

The ^{1}H-^{13}C cross signals presented in the HSQC spectra were assigned by contrasting it with literature data (Ibarra et al., 2007; Wen et al., 2015, 2012; Yuan et al., 2011; Zhang et al., 2010). All assignments are depicted in Table S6 and cross signals from the different lignin subunits, including alkyl-aryl ether structures (β-O-4), resinols (β-β), phenylcoumaran (β-1), spirodienone (β-5) among others, are shown in Fig. 6. The identification of some of these subunits was also confirmed by 2D HMBC NMR technique (data not shown).

At first glance, both HSQC regions from native Kraft lignin and HEAP lignin (Fig. 6) as well as HEAF and THEAP lignins (Figure S22 in ESI) presented the same cross signals. This is indicative of null or low chemical modification of main inter-unit linkages present in lignin structure, confirming FTIR results. Nevertheless, a semi-quantitative analysis was attempted to stress out the effect of each PIL on the relative abundance of identified lignin subunits after its dissolution/precipitation steps. The obtained data is depicted in Table 2.

The HSQC semi-quantitative characterization of the side chains of native Kraft lignin structure demonstrated a high abundance in β-O-4 alkyl-aryl ether (48.6 %) and β-β resinol subunits (35.8 %). On the other hand, phenylcoumaran (2.6 %) and spirodienone (8.6 %) substructures represent a lower fraction of lignin. The remaining content (4.4 %) refers to *p*-hydroxycinnamyl derived subunits. These results are in agreement with literature data shown by NMR analysis of other Kraft lignins from *E. globulus* wood (Martinez et al., 2010). The relative

analysis between each sample demonstrated that treating native Kraft lignin with PILs at 393.15 K followed by its precipitation have only a minor impact on its composition. In all cases, β-O-4 alkyl-ether substructures content in recovered lignins increased (between 13.1 and 34.4 % increase), while the opposite was observed for other lignin subunits, especially for β-β resinol type (between 10.6 and 33.4 % reduction).

A major difference observed in β-O-4 and β-β contents can be contrasted with literature data and correlated with GPC results. Ragauskas et al. have shown in a recent study based on lignin fractionation by organic solvents (Wang et al., 2018) that high molecular weight lignin molecules tend to possess more β-O-4 linkages, while the subunits of oligomeric lignin molecules are preferably linked through C—C bonds (as consequence of intense α-O-4 and β-O-4 ether cleavage). As aforementioned, the treatment with PILs allowed the removal of low molecular weight lignin molecules, leading to a slight increase of Mw, Mn and PDI of the recovered lignin samples. Therefore, the reduction of β-β resinol subunits in lignin structure could be explained by this behavior. Although HSQC semi-quantitative analysis demonstrated differences in lignin structure between native Kraft lignin and PILs samples, this should be looked as little modification in agreement with GPC and FTIR results. It can be stated that lignin dissolution mechanism in examined PILs is mostly governed by the disruption of the intramolecular bonding of lignin macromolecules and the establishment of intermolecular non-covalent bonds with PILs, specially with the anionic part.

Regarding the PIL contamination in recovered lignin samples, NMR spectra showed very low intensity of characteristic chemical shifts from HEAF (δ_C/δ_H 40/3.20) and HEAP (δ_C/δ_H 42/3.15). On the contrary, the contamination of THEAP in recovered lignin was higher and it was identified as multiple derived compounds from esterification between the three hydroxyl groups in tris(2-hydroxyethyl)amine and propionic acid. This is in agreement with FTIR spectrum obtained for THEAP lignin showing the appearance of a vibrational band at 1725 cm^{-1} associated to C=O stretching in ester groups.

3.5. Recycling of PIL

The recycling of ILs are fundamental to obtain a sustainable and economical process. To achieve this goal, an easy way to extract lignin from lignocellulosic biomass is needed and afterwards an efficient separation of lignin from the IL medium is of utmost importance. In this work, we demonstrated the recovery of HEAP using distillation and evaporation under reduced pressure. Particularly, the recovery of HEAP is beneficial as it presents high and similar lignin solubility for neat PIL and for PIL at 15 wt% water content, while negligible lignin solubility is noticed for water content higher than 75 wt% (Fig. 3). This means that PIL with low water content can be used, avoiding a prior PIL drying step, and practically all lignin dissolved in the PIL can be precipitated with the addition of water. The key step comes with an efficient water evaporation. The recovered solvent was first submitted to a distillation process at ambient pressure achieving approximately 41 wt% water content, where no vapor was observed after this point. Afterwards, the solution was submitted to a vacuum evaporation process (333.15 K and 10 kPa for 1 h) to remove the remaining water and to reach 15 wt% water content. This method allowed successful HEAP recovery up to 95 % of the initial IL mass.

Lignin solubility in recovered HEAP (15 wt% water content) was then examined up to three cycles of PIL recovery/reuse. The solubility efficiencies contrasting to neat PIL were 99.6, 99.1 and 98.7 % for recycling cycles 1, 2 and 3, respectively (Fig. 7). Only a very minor decrease in the dissolution efficiency was observed in these recycle assays, showing that HEAP can be reused without significantly losing its performance.
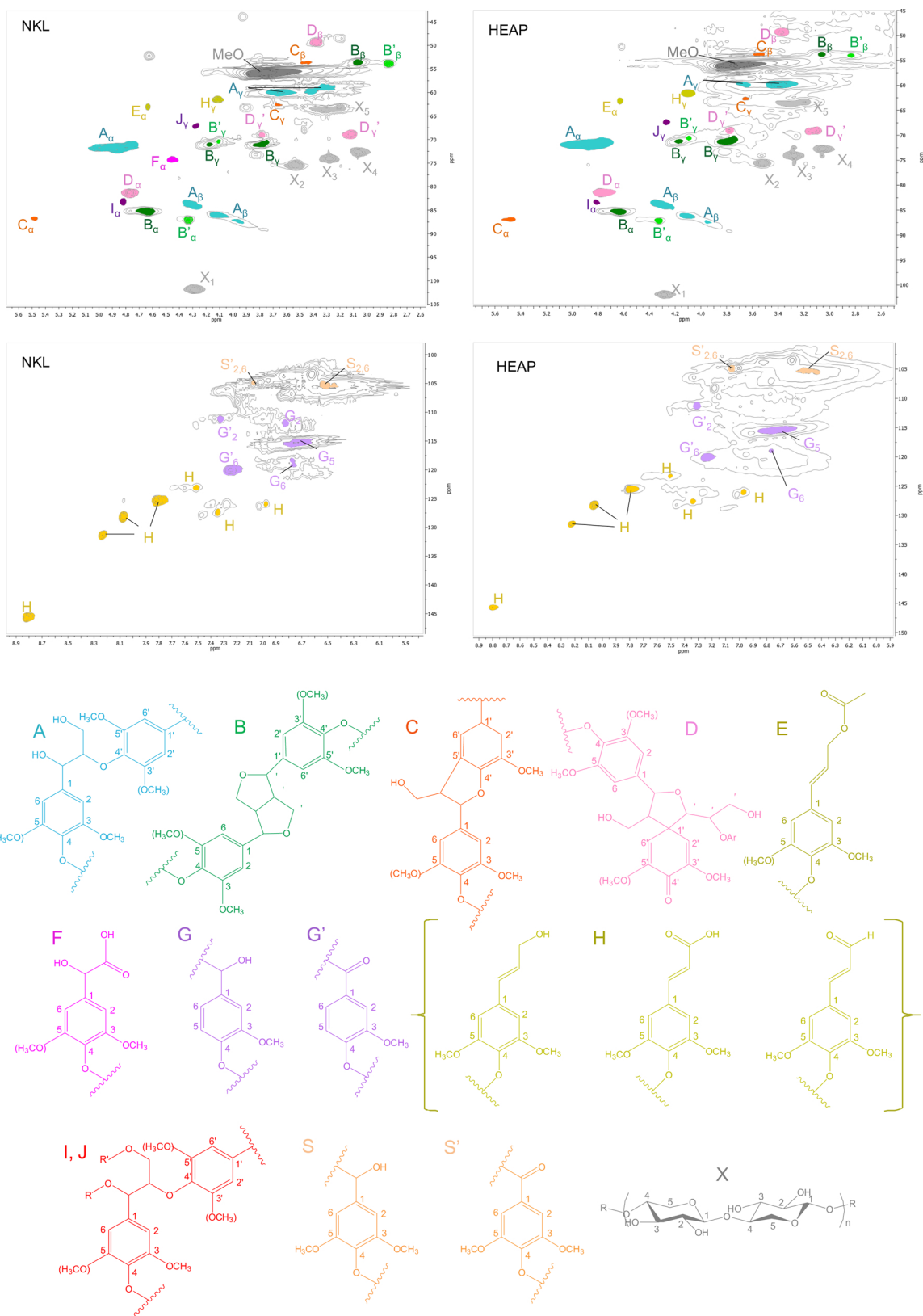
Fig. 6. 2D HSQC NMR of native Kraft lignin (NKL) and recovered lignin from HEAP (393.15 K) with corresponding ^{13}C-^{1}H cross signal assignments to main lignin subunits. The lignin substructures are the following: (A) β-O-4' linkages; (B) Resinol (β-β'); (C) Phenylcoumaran (β-5'); (D) Spirodienone (β-1'); (E) cinnamyl acetate end-groups; (F) Ar-CHOH-COOH unit (C_α-H_α); (G) Guaiacyl unit; (G') oxidized Guaiacyl unit with a C_α ketone or carboxyl group; (H) p-hydroxycynnamyl alcohol, aldehyde or carboxylic (aromatic and end groups); (I) β-O-4' substructure C_α etherified to carbohydrate (R, polysaccharide; R', H); (J) β-O-4' substructure C_γ etherified to carbohydrate (R, H; R', polysaccharide); ($S_{2,6}$) Syringyl unit; ($S'_{2,6}$) oxidized syringyl unit with a C_α ketone (phenolic); (X) Xylan.

Table 2
Relative abundance of main inter-unit linkages and lignin substructures as a percentage of total side chains from integration of ^{13}C-^{1}H cross signals in the HSQC spectra of native Kraft lignin and recovered lignins from PILs.

Linkage (Substructure) Type	Relative abundance % ([a])			
	Native Kraft lignin	HEAF lignin	HEAP lignin	THEAP lignin
β-O-4 (A)	48.6 (0.0)	62.7 (+22.5)	65.3 (+34.4)	55.0 (+13.1)
β-β (B)	35.8 (0.0)	25.5 (−28.8)	23.8 (−33.4)	32.0 (−10.6)
β-5 (C)	2.6 (0.0)	2.5 (−5.4)	2.2 (−15.3)	1.3 (-50.0)
β-1 (D)	8.6 (0.0)	5.6 (−34.8)	5.6 (−35.3)	7.8 (−9.4)
Others	4.4 (0.0)	3.7 (−15.3)	3.1 (−30.7)	3.9 (−10.9)

[a] Relative percentage deviation contrasting to the initial native Kraft lignin content.
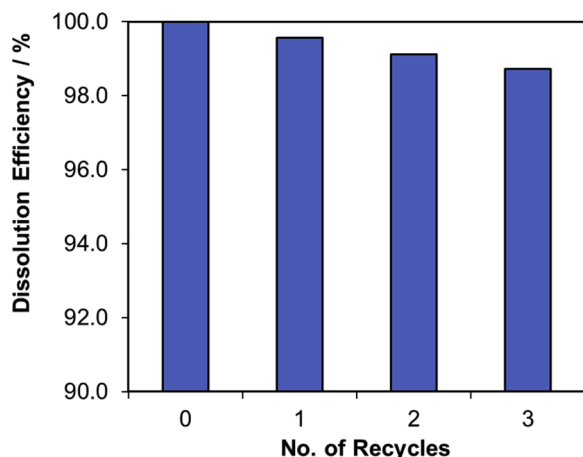

Fig. 7. Dissolution efficiency of lignin in HEAP (85 wt%) and recycled HEAP (85 wt%).

4. Conclusions

This work demonstrates the outstanding ability of alkylammonium PILs and their aqueous solutions to dissolve Kraft lignin at low temperature. The anion showed to play a major role in lignin dissolution than the cationic counterpart. The smaller cation with lower number of hydroxyalkyl groups favored the lignin dissolution process. On the other hand, the larger the alkyl carbon chain of the anion, the higher is the solubility of lignin in PIL. The results show that the presence of water is an important factor affecting the capacity of the PIL to dissolve this macromolecule. In general, the addition of water has a negative influence on the solubility process. Amongst examined solvents, hexanoate-based PIL (HEAH) presented the best performance for Kraft lignin dissolution allowing 37.7 wt% solubility at 323.15 K. On the other hand, HEAO stands as an exception, where the octanoate anion acts as hydrotropic agent promoting the lignin dissolution in water with a maximum solubility value at 40 wt% water content. A sharp decrease was observed using HEAF and HEAA as solvent media, while HEAP and HEAH present a softer reduction on lignin solubility with the addition of water. Regarding the temperature effect, the lignin dissolution was favored by temperature increase revealing the endothermic nature of the lignin dissolution process.

A comprehensive characterization of recovered lignin samples was performed after submitting lignin at 393.15 K for 6 h in selected PILs. As major conclusion, the molecular weight and relative abundance of lignin subunits slightly changed between native Kraft lignin and recovered lignin samples and seems to be connected. However, the modification is minimal, making PILs excellent non-derivatizing solvents of lignin. Moreover, consecutive steps of simple distillation and evaporation under reduced pressure allowed up to 95 % PIL recovery and the reuse of the solvent was accomplished for at least 3 cycles without losing its performance.

The disclosed results demonstrate a massive potential of PILs for application in biomass delignification and lignin dissolution processes and are in the way to accomplish higher sustainability in lignin valorization than traditional technologies.

Declaration of Competing Interest

None.

Appendix A. Supplementary data

Supplementary material related to this article can be found, in the online version, at doi:https://doi.org/10.1016/j.indcrop.2019.111866.

References

Achinivu, E.C., 2018. Protic ionic liquids for lignin extraction—a lignin characterization study. Int. J. Mol. Sci. 19, 428. https://doi.org/10.3390/ijms19020428.

Achinivu, E.C., Howard, R.M., Li, G., Gracz, H., Henderson, W.A., 2014. Lignin extraction from biomass with protic ionic liquids. Green Chem. 16, 1114–1119. https://doi.org/10.1039/c3gc42306a.

Akiba, T., Tsurumaki, A., Ohno, H., 2017. Induction of lignin solubility for a series of polar ionic liquids by the addition of a small amount of water. Green Chem. 19, 2260–2265. https://doi.org/10.1039/c7gc00626h.

Álvarez, V.H., Dosil, N., Gonzalez-Cabaleiro, R., Mattedi, S., Martin-Pastor, M., Iglesias, M., Navaza, J.M., 2010. Brønsted ionic liquids for sustainable processes: synthesis and physical properties. J. Chem. Eng. Data 55, 625–632. https://doi.org/10.1021/je900550v.

Brandt, A., Chen, L., Van Dongen, B.E., Welton, T., Hallett, J.P., 2015. Structural changes in lignins isolated using an acidic ionic liquid water mixture. Green Chem. 17, 5019–5034. https://doi.org/10.1039/c5gc01314c.

Brandt-Talbot, A., Gschwend, F.J.V., Fennell, P.S., Lammens, T.M., Tan, B., Weale, J., Hallett, J.P., 2017. An economically viable ionic liquid for the fractionation of lignocellulosic biomass. Green Chem. 19, 3078–3102. https://doi.org/10.1039/c7gc00705a.

Cachet, N., Camy, S., Benjelloun-Mlayah, B., Condoret, J.S., Delmas, M., 2014. Esterification of organosolv lignin under supercritical conditions. Ind. Crops Prod. 58, 287–297. https://doi.org/10.1016/j.indcrop.2014.03.039.

Cademartori, P.H.G., dos Santos, P.S.B., Serrano, L., Labidi, J., Gatto, D.A., 2013. Effect of thermal treatment on physicochemical properties of Gympie messmate wood. Ind.

Crops Prod. 45, 360–366. https://doi.org/10.1016/j.indcrop.2012.12.048.

Chambon, C.L., Mkhize, T.Y., Reddy, P., Brandt-Talbot, A., Deenadayalu, N., Fennell, P.S., Hallett, J.P., 2018. Pretreatment of South African sugarcane bagasse using a low-cost protic ionic liquid: a comparison of whole, depithed, fibrous and pith bagasse fractions. Biotechnol. Biofuels 11, 247. https://doi.org/10.1186/s13068-018-1247-0.

Chang, W.R., Hwang, J.J., Wu, W., 2017. Environmental impact and sustainability study on biofuels for transportation applications. Renew. Sustain. Energy Rev. 67, 277–288. https://doi.org/10.1016/j.rser.2016.09.020.

Cláudio, A.F.M., Neves, M.C., Shimizu, K., Canongia Lopes, J.N., Freire, M.G., Coutinho, J.A.P., 2015. The magic of aqueous solutions of ionic liquids: ionic liquids as a powerful class of catanionic hydrotropes. Green Chem. 17, 3948–3963. https://doi.org/10.1039/c5gc00712g.

Da Costa Lopes, A.M., Bogel-Lukasik, R., 2015. Acidic ionic liquids as sustainable approach of cellulose and lignocellulosic biomass conversion without additional catalysts. ChemSusChem 8, 947–965. https://doi.org/10.1002/cssc.201402950.

Dahmen, N., Lewandowski, I., Zibek, S., Weidtmann, A., 2019. Integrated lignocellulosic value chains in a growing bioeconomy: status quo and perspectives. GCB Bioenergy 11, 107–117. https://doi.org/10.1111/gcbb.12586.

Fathi-Azarjbayjani, A., Mabhoot, A., Martínez, F., Jouyban, A., 2016. Modeling, solubility, and thermodynamic aspects of sodium phenytoin in propylene glycol-water mixtures. J. Mol. Liq. 219, 68–73. https://doi.org/10.1016/j.molliq.2016.02.089.

Fernández-Costas, C., Gouveia, S., Sanromán, M.A., Moldes, D., 2014. Structural characterization of Kraft lignins from different spent cooking liquors by 1D and 2D Nuclear Magnetic Resonance spectroscopy. Biomass Bioenergy 63, 156–166. https://doi.org/10.1016/j.biombioe.2014.02.020.

García, A., Erdocia, X., González Alriols, M., Labidi, J., 2012. Effect of ultrasound treatment on the physicochemical properties of alkaline lignin. Chem. Eng. Process. Process Intensif. 62, 150–158. https://doi.org/10.1016/j.cep.2012.07.011.

Glas, D., Van Doorslaer, C., Depuydt, D., Liebner, F., Rosenau, T., Binnemans, K., De Vos, D.E., 2015. Lignin solubility in non-imidazolium ionic liquids. J. Chem. Technol. Biotechnol. 90, 1821–1826. https://doi.org/10.1002/jctb.4492.

Gordobil, O., Delucis, R., Egüés, I., Labidi, J., 2015. Kraft lignin as filler in PLA to improve ductility and thermal properties. Ind. Crops Prod. 72, 46–53. https://doi.org/10.1016/j.indcrop.2015.01.055.

Hart, W.E.S., Harper, J.B., Aldous, L., 2015. The effect of changing the components of an ionic liquid upon the solubility of lignin. Green Chem. 17, 214–218. https://doi.org/10.1039/c4gc01846e.

Hou, X.D., Xu, J., Li, N., Zong, M.H., 2015. Effect of anion structures on cholinium ionic liquids pretreatment of rice straw and the subsequent enzymatic hydrolysis. Biotechnol. Bioeng. 112, 65–73. https://doi.org/10.1002/bit.25335.

Hu, J., Zhang, Q., Lee, D.J., 2018. Kraft lignin biorefinery: a perspective. Bioresour. Technol. 247, 1181–1183. https://doi.org/10.1016/j.biortech.2017.08.169.

Ibarra, D., Chávez, M.I., Rencoret, J., Del Río, J.C., Gutiérrez, A., Romero, J., Camarero, S., Martínez, M.J., Jiménez-Barbero, J., Martínez, A.T., 2007. Lignin modification during Eucalyptus globulus kraft pulping followed by totally chlorine-free bleaching: a two-dimensional nuclear magnetic resonance, Fourier transform infrared, and pyrolysis-gas chromatography/mass spectrometry study. J. Agric. Food Chem. 55, 3477–3490. https://doi.org/10.1021/jf063728t.

Iglesias, M., Gonzalez-Olmos, R., Cota, I., Medina, F., 2010. Brønsted ionic liquids: study of physico-chemical properties and catalytic activity in aldol condensations. Chem. Eng. J. 162, 802–808. https://doi.org/10.1016/j.cej.2010.06.008.

Ji, W., Ding, Z., Liu, J., Song, Q., Xia, X., Gao, H., Wang, H., Gu, W., 2012. Mechanism of lignin dissolution and regeneration in ionic liquid. Energy Fuel 26, 6393–6403. https://doi.org/10.1021/ef301231a.

Kim, K.H., Oh, H.K., Heo, B., Kim, N.A., Lim, D.G., Jeong, S.H., 2018. Solubility evaluation and thermodynamic modeling of β-lapachone in water and ten organic solvents at different temperatures. Fluid Phase Equilib. 472, 1–8. https://doi.org/10.1016/j.fluid.2018.05.005.

Liitiä, T.M., Maunu, S.L., Hortling, B., Toikka, M., Kilpeläinen, I., 2003. Analysis of technical lignins by two- and three-dimensional NMR spectroscopy. J. Agric. Food Chem. 51, 2136–2143. https://doi.org/10.1021/jf0204349.

Long, B., Xia, Y., Deng, Z., Ding, Y., 2017. Understanding the enhanced solubility of 1,3-benzenedicarboxylic acid in polar binary solvents of (acetone + water) at various temperatures. J. Chem. Thermodyn. 105, 105–111. https://doi.org/10.1016/j.jct.2016.10.011.

Martinez, A.T., Nieto, L., Kim, H., Gutierrez, A., Rencoret, J., Jimenez-Barbero, J., Faulds, C.B., Ralph, J., del Rio, J.C., 2010. Lignin composition and structure in young versus adult Eucalyptus globulus plants. Plant Physiol. 155, 667–682. https://doi.org/10.1104/pp.110.167254.

Merino, O., Fundora-Galano, G., Luque, R., Martínez-Palou, R., 2018. Understanding microwave-assisted lignin solubilization in protic ionic liquids with multiaromatic imidazolium cations. ACS Sustain. Chem. Eng. 6, 4122–4129. https://doi.org/10.1021/acssuschemeng.7b04535.

Miranda, R., Neta, J.V., Romanholo Ferreira, L.F., Gomes, W.A., do Nascimento, C.S., de B. Gomes, E., Mattedi, S., Soares, C.M.F., Lima, Á.S., 2019. Pineapple crown delignification using low-cost ionic liquid based on ethanolamine and organic acids. Carbohydr. Polym. 206, 302–308. https://doi.org/10.1016/j.carbpol.2018.10.112.

Mu, L., Shi, Y., Chen, L., Ji, T., Yuan, R., Wang, H., Zhu, J., 2015. [N-Methyl-2-pyrrolidone][C1-C4 carboxylic acid]: a novel solvent system with exceptional lignin solubility. Chem. Commun. 51, 13554–13557. https://doi.org/10.1039/c5cc04191k.

Nevrez, L.A.M., Casarrubias, L.B., Celzard, A., Fierro, V., Müoz, V.T., Davila, A.C., Lubian, J.R.T., Snchez, G.G., 2011. Biopolymer-based nanocomposites: effect of lignin acetylation in cellulose triacetate films. Sci. Technol. Adv. Mater. 12, 045006. https://doi.org/10.1088/1468-6996/12/4/045006.

Pandey, K.K., Pitman, A.J., 2003. FTIR studies of the changes in wood chemistry following decay by brown-rot and white-rot fungi. Int. Biodeterior. Biodegrad. 52, 151–160. https://doi.org/10.1016/S0964-8305(03)00052-0.

Popescu, C.-M., Vasile, C., Popescu, M.-C., Singurel, G., Munteanu, B.S., Popa, V.I., 2006. Analytical methods for lignin characterisation. II) Spectroscopical studies. Cell. Chem. Technol. 40, 597–622.

Prado, R., Erdocia, X., Labidi, J., 2013. Lignin extraction and purification with ionic liquids. J. Chem. Technol. Biotechnol. 88, 1248–1257. https://doi.org/10.1002/jctb.3965.

Pu, Y., Jiang, N., Ragauskas, A.J., 2007. Ionic liquid as a green solvent for lignin. J. Wood Chem. Technol. 27, 23–33. https://doi.org/10.1080/02773810701282330.

Ralph, J., Landucci, L., 2010. NMR of lignins. Lignin and Lignans. https://doi.org/10.1201/ebk1574444865-c5.

Rashid, T., Kait, C.F., Regupathi, I., Murugesan, T., 2016. Dissolution of kraft lignin using protic ionic liquids and characterization. Ind. Crops Prod. 84, 284–293. https://doi.org/10.1016/j.indcrop.2016.02.017.

Rashid, T., Gnanasundaram, N., Appusamy, A., Kait, C.F., Thanabalan, M., 2018. Enhanced lignin extraction from different species of oil palm biomass: kinetics and optimization of extraction conditions. Ind. Crops Prod. 116, 122–136. https://doi.org/10.1016/j.indcrop.2018.02.056.

Semerci, I., Güler, F., 2018. Protic ionic liquids as effective agents for pretreatment of cotton stalks at high biomass loading. Ind. Crops Prod. 125, 588–595. https://doi.org/10.1016/j.indcrop.2018.09.046.

Silveira, M.H.L., Morais, A.R.C., Da Costa Lopes, A.M., Olekszyszen, D.N., Bogel-Łukasik, R., Andreaus, J., Pereira Ramos, L., 2015. Current pretreatment technologies for the development of cellulosic ethanol and biorefineries. ChemSusChem 8 (20), 3366–3390. https://doi.org/10.1002/cssc.201500282.

Soares, B., Tavares, D.J.P., Amaral, J.L., Silvestre, A.J.D., Freire, C.S.R., Coutinho, J.A.P., 2017. Enhanced solubility of lignin monomeric model compounds and technical lignins in aqueous solutions of deep eutectic solvents. ACS Sustain. Chem. Eng. 5, 4056–4065. https://doi.org/10.1021/acssuschemeng.7b00053.

Soares, B., Silvestre, A.J.D., Rodrigues Pinto, P.C., Freire, C.S.R., Coutinho, J.A.P., 2019. Hydrotropy and cosolvency in lignin solubilization with deep eutectic solvents. ACS Sustain. Chem. Eng. 7, 12485–12493. https://doi.org/10.1021/acssuschemeng.9b02109.

Sun, S.N., Li, M.F., Yuan, T.Q., Xu, F., Sun, R.C., 2012. Sequential extractions and structural characterization of lignin with ethanol and alkali from bamboo (Neosinocalamus affinis). Ind. Crops Prod. 37, 51–60. https://doi.org/10.1016/j.indcrop.2011.11.033.

Tolbert, Allison, Akinosho, Hannah, Khunsupat, Ratayakorn, Naskar, Amit K., Ragauskas, Arthur J., 2014. Characterization and analysis of the molecular weight of lignin. Biofuels Bioprod. Biorefining 8, 836–856. https://doi.org/10.1002/bbb.1500.

Wang, Y.Y., Li, M., Wyman, C.E., Cai, C.M., Ragauskas, A.J., 2018. Fast fractionation of technical lignins by organic cosolvents. ACS Sustain. Chem. Eng. 6, 6064–6072. https://doi.org/10.1021/acssuschemeng.7b04546.

Welton, T., 2018. Ionic liquids: a brief history. Biophys. Rev. 10, 691–706. https://doi.org/10.1007/s12551-018-0419-2.

Wen, J.L., Xue, B.L., Xu, F., Sun, R.C., 2012. Unveiling the structural heterogeneity of bamboo lignin by in situ HSQC NMR technique. Bioenergy Res. 5, 886–903. https://doi.org/10.1007/s12155-012-9203-5.

Wen, J.L., Sun, S.L., Yuan, T.Q., Sun, R.C., 2015. Structural elucidation of whole lignin from Eucalyptus based on preswelling and enzymatic hydrolysis. Green Chem. 17, 1589–1596. https://doi.org/10.1039/c4gc01889c.

Xu, A., Guo, X., Zhang, Y., Li, Z., Wang, J., 2017. Efficient and sustainable solvents for lignin dissolution: aqueous choline carboxylate solutions. Green Chem. 19, 4067–4073. https://doi.org/10.1039/c7gc01886j.

Yuan, T.Q., Sun, S.N., Xu, F., Sun, R.C., 2011. Characterization of lignin structures and lignin-carbohydrate complex (LCC) linkages by quantitative13C and 2D HSQC NMR spectroscopy. J. Agric. Food Chem. 59, 10604–10614. https://doi.org/10.1021/jf2031549.

Zhang, A., Lu, F., Sun, R.C., Ralph, J., 2010. Isolation of cellulolytic enzyme lignin from wood preswollen/dissolved in dimethyl sulfoxide/N-methylimidazole. J. Agric. Food Chem. 58, 3446–3450. https://doi.org/10.1021/jf903998d.

Zhang, Y., He, H., Dong, K., Fan, M., Zhang, S., 2017. A DFT study on lignin dissolution in imidazolium-based ionic liquids. RSC Adv. 7, 12670–12681. https://doi.org/10.1039/c6ra27059j.

Zhu, X., Peng, C., Chen, H., Chen, Q., Zhao, Z.K., Zheng, Q., Xie, H., 2018. Opportunities of ionic liquids for lignin utilization from biorefinery. ChemistrySelect 3, 7945–7962. https://doi.org/10.1002/slct.201801393.